

High Thermal Conductivity and Reliability, Downsized IGBT Module for Automotive Applications

Fumio Nagaune, Shinichiro Adachi, Takahisa Hitachi, Hiromichi Gohara,
Akira Morozumi, and Akira Nishiura
Fuji Electric Co., Ltd
4-18-1, Tsukama, Matsumoto City, Nagano, 390-0821 Japan
email: nagaune-fumio@fujielectric.co.jp

Abstract

Recently, electromotive system of automotive has dramatically progressed. Highly reliable and compact IGBT module is required for automotive application. We have developed a new 6-pack IGBT module and downsized system with high thermal conductivity and high reliability. To achieve high thermal conductivity, direct liquid cooling fin and liquid jacket structure have been optimized and thermal conductivity of the internal insulating structure in the IGBT module has been improved. To achieve high reliability, crack growth in solder layers of IGBT module has been reduced by solder material. In this paper, we have described about the optimization results of the cooling liquid system for the new IGBT module and the experimental results with several solder materials to realize longer car lifetime. Furthermore, the estimation and some test results about the reliability of the new 6-pack IGBT module have been described.

Keywords: IGBT module, direct liquid cooling, liquid jacket, reliability

1 Introduction

Recently, electromotive system of automotive has dramatically progressed for promotion of zero emission and low-fuel consumption. HEV/EV (Hybrid Electric Vehicle/Electric Vehicle) demand is increasing progressively and electrical stress of vehicle is also increasing. Therefore, downsizing, cost reduction and higher power density of PCU (Power Control Unit) for HEV/EV system are required. IGBT module is a main component in PCU for motor drive and boost converter system. It is strongly required downsizing, higher power density and improving cooling capability.

From the above requirements of the HEV/EV applications, we have developed the new 6-pack IGBT module with high thermal conductivity,

high reliability and downsized direct liquid cooling system. The direct liquid cooling fin and the liquid jacket structure have been optimized and the internal insulating structure of the IGBT module has been improved to achieve high thermal conductivity. Furthermore, the crack growth in solder layers of the IGBT modules has reduced to achieve longer lifetime by improvement of the solder material.

In this paper, the optimization results of the cooling fin and liquid jacket structure and the experimental results of the internal insulating material of the IGBT module are described. The evaluation results with several solder materials to consider longer lifetime are also described. Furthermore, the estimation and some test results about the reliability of the new 6-pack IGBT module are described.

2 Newly developed direct liquid cooling 6-pack IGBT module

2.1 Advantage of direct liquid cooling fin system

Figure 1 shows the cross section of the conventional indirect cooling system and the newly developed direct liquid cooling system. In the case of indirect liquid cooling systems, the IGBT module is normally mounted onto the aluminum cooling fin with the thermal grease layer between base plate of the IGBT module and aluminum cooling fin. In this system, the thermal resistance of the thermal grease layer and the insulated substrate are higher than that of the other material of the IGBT module. It prevents IGBT/FWD die and module sizes from downsizing due to its high thermal resistance.

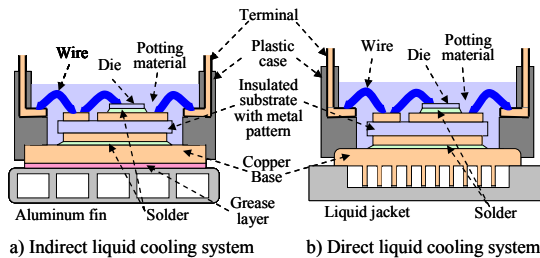


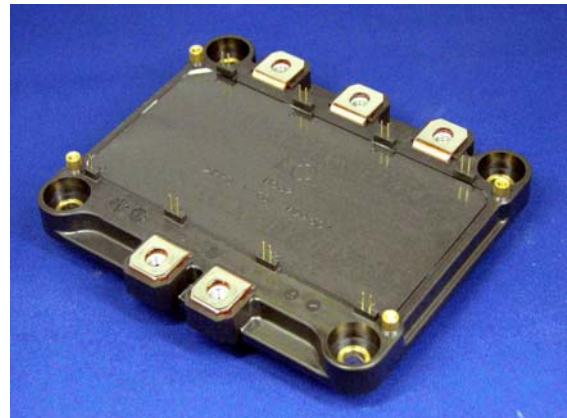
Figure 1: Cross section of IGBT module

On the other hand, in the case of direct liquid cooling system, the thermal grease layer is eliminated. The thermal resistance of the heat sink is decreased by using fin base made of high thermal conductivity material, such as copper instead of aluminum. Therefore, the direct liquid cooling system enables downsizing of the IGBT module and cooling system dramatically. We have developed a small size and high thermal conductivity IGBT module by direct cooling fin structure with copper fin base.

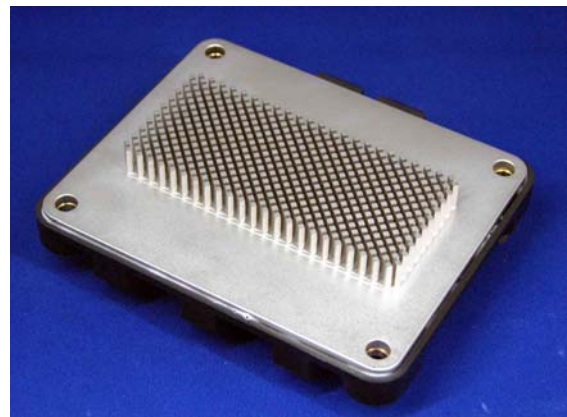
2.2 Outline of the newly developed direct liquid cooling IGBT module

Figure 2 shows pictures of the newly developed 6-pack 650V/600A direct liquid cooling IGBT module. We have already developed a 6-pack 650V/400A of the same circuit configuration [1]. This IGBT module is suitable for inverter application for mild HEV and EV. The newest generation chip technology "V-series" [2] is used in the newly developed IGBT module. The copper base has a lot of square pin fins and cooling liquid flows directly in the pin fin area.

The direct liquid cooling fin system enables current rating 600A/die and downsizing as 131mm x 113mm device size for 650V/600A 6-pack IGBT module.



a) Terminal side of IGBT module



b) Fin base side of IGBT module

Figure 2: Newly developed 6-pack 650V/600A direct liquid cooling IGBT module

The dimensions of width, height and interval of each square pin fins have optimized under the thermal conductivity performance and assembly method. The round pin fin structure is the most general used for direct cooling fin structure [3], [4], [5]. However, the square pin fin structure has a larger surface area than that of the round pin fin. Therefore, the thermal resistance of the square pin fin structure is lower than that of the round pin fin structure [1]. Furthermore, the square pin fin is assembled easily by cutting or pressing. The square pin fin of the new IGBT module has minimum dimension as considering the assembly method.

Figure 3 shows the relative thermal resistance compared with the indirect and direct liquid cooling system with the copper base. The aluminum oxide(AlO) insulated substrate is used in the conventional IGBT module. The silicon nitride(SiN) insulated substrate has been applied for the newly developed IGBT module for the purpose of thermal resistance decreasing. In the case of the conventional IGBT module, the thermal resistance of the thermal grease and the AlO insulated substrate are dominant in total thermal resistance. In contrast, the direct liquid cooling system does not have the thermal grease layer and the thermal resistance of the SiN insulated substrate is about 30% of the AlO insulated substrate. Therefore, the total thermal resistance has been decreased to 40% by using high thermal conductivity SiN insulated substrate.

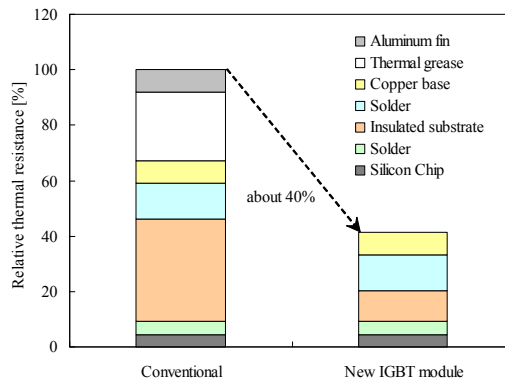


Figure 3: Comparison of relative thermal resistance

3 Optimization of direct liquid cooling system for the newly developed IGBT module

In the case that IGBT module is used for inverter application of mild HEV and EV, the smoothing capacitor(DC bus capacitor) is connected to the P/N terminals and the AC output bus bar is connected to the AC terminals. Generally, the current sensors are inserted with the AC bus bar. Therefore, the cooling liquid jacket structure should be studied in consideration of shape and layout of the smoothing capacitor, the AC output bus bar, and the current sensors in PCU system. Figure 4 shows the typical layout of the newly developed IGBT module, the smoothing capacitor, the control circuit boards, the current sensor, and the output terminal. In this section, the optimization result of the liquid cooling

jacket structure for the newly developed IGBT module is described.

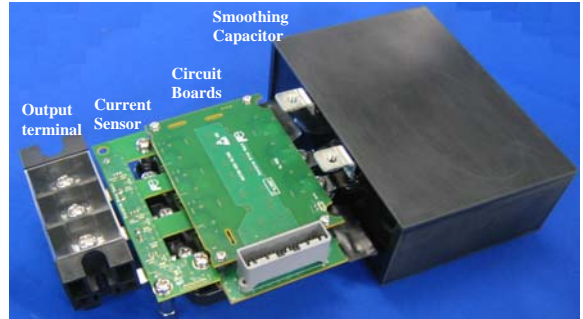


Figure 4: Typical layout of IGBT module, smoothing capacitor, control circuit boards, current sensor, and output terminal

3.1 Inlet/outlet layout and cooling liquid flow direction design

Figure 5 shows the several cases about the cooling liquid inlet/outlet layout and the cooling liquid flow direction.

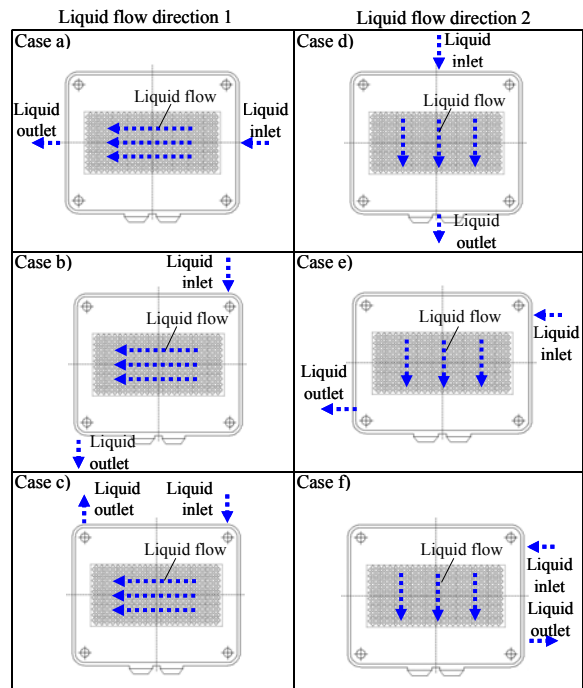


Figure 5: Several cases about liquid inlet/outlet layout and liquid flow direction

In consideration of the cooling liquid flow direction in the pin fin area, two liquid flow directions are generally applied in PCU system as shown in Figure 5. Regarding the cooling liquid inlet/outlet layout, three inlet/outlet layouts are

considered in the PCU system as shown in Figure 5, too.

The direction 1 is a major (long) axis liquid flow, and the direction 2 is a minor (short) axis liquid flow. In the case of the liquid flow direction 1, the relative flow velocity is a little higher than that of the liquid flow direction 2 because of shorter flow width. Therefore, the pressure loss of direction 1 is larger than that of direction 2. It is necessary that the pressure loss should be reduced in the case of liquid flow direction 1. On the other hand, in the case of the liquid flow direction 2, the uniform flow velocity should be considered, because the flow width is wider than direction 1. As the point of view about the cooling liquid inlet/outlet layout, the cooling liquid inlet/outlet pipes should be located to avoid the smoothing capacitor and the current sensors.

3.2 Optimized cooling liquid jacket structure design

For the optimization of the liquid jacket structure, velocity vector of flowing liquid, pressure loss, and junction temperature are analyzed with thermal liquid simulator "Icepak". The LLC (Long Life Coolant) is used for a cooling liquid. Figure 6 shows the internal layout of the newly developed 650V/400A IGBT module for a simulation. The insulated substrate is separated into three parts by each phase, and each insulated substrate has two IGBT dies and two FWD dies. The square pin fins are located under the insulated substrate area.

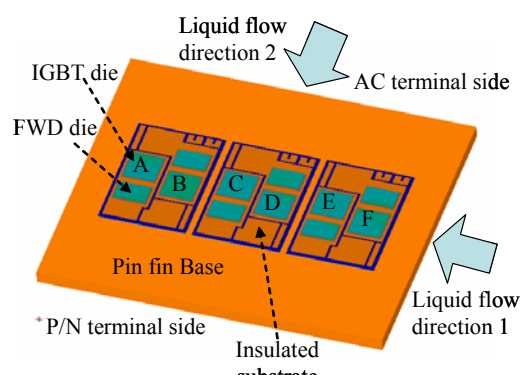
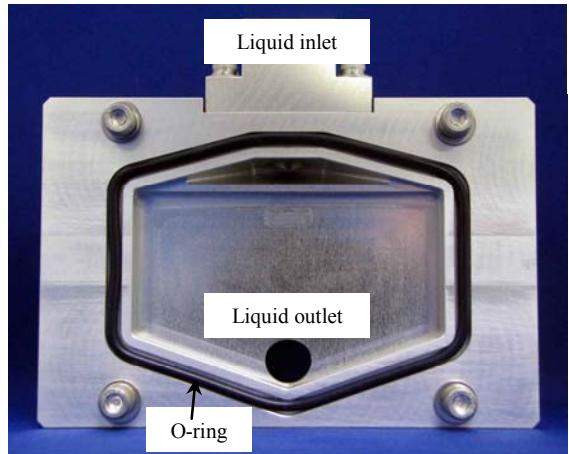


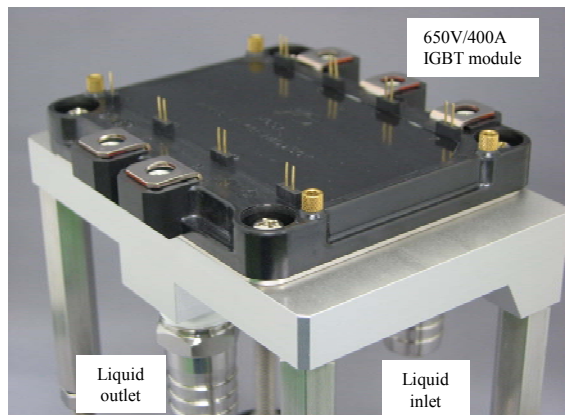
Figure 6: Internal layout of the newly developed 650V/400A IGBT module

Figure 7 shows the optimized cooling liquid jacket for the newly developed 650V/400A IGBT module. The pressure loss in the case of the cooling liquid flow direction 1 is a little high

because of the longer flow length. In the case of b), c), e) and f) inlet/outlet layout, the cooling liquid flow direction and the inlet/outlet axis are cross at right angle. Therefore, the pressure loss in these cases is a little high, too. Furthermore, In the case of c) and f) inlet/outlet layout, the local rotating liquid flow will be generated easily in the cooling liquid jacket [1].



a) Prototype of cooling liquid jacket



b) Prototype of cooling liquid jacket and 650V/400A 6-pack IGBT module

Figure 7: Optimized liquid jacket for the newly developed 650V/400A IGBT module

From these analysis results, the case d) as shown in Figure 5 has better liquid flow distribution and lower pressure loss. This structure is applied to the cooling liquid jacket for the newly developed IGBT module. The inlet/outlet pipes are connected to the bottom surface of the cooling liquid jacket for the purpose of avoiding the smoothing capacitor and the current sensor.

For the purpose of getting constant and uniform liquid flow, the inlet and outlet pipes are located

on the middle of the AC terminal side and the P/N terminal side. The liquid flow area is hexagonal shape to spread the cooling liquid symmetrically and uniformly in the square pin fin area.

Figure 8 shows the simulation results of the relative flow velocity distribution at the optimized cooling liquid jacket structure for the newly developed IGBT module. The cooling liquid flow in the square pin fin area is almost constant and uniform.

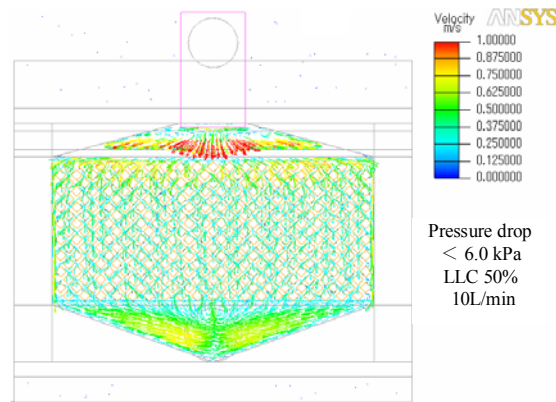


Figure 8: Relative flow velocity distribution

Table 1 shows the comparison results about the junction temperatures of IGBT dies calculated from the thermal liquid simulation and the actual measurement.

Table 1: Comparison results about junction temperatures of IGBT dies

IGBT chip No	A	B	C	D	E	F
Simulation results [°C]	133.6	137.6	138.4	139.1	136.6	137.7
Measurement results [°C]	136.7	137.4	137.1	137.6	136.9	136.9
Difference [%]	2.3	0.1	0.9	1.1	0.2	0.6

Conditions:
 Power dissipation loss of IGBT : 258W
 Cooling liquid : LLC50%
 Cooling liquid flow rate : 10L/minute
 Cooling liquid temperature : 65°C

The junction temperature calculated from the thermal liquid simulation is good agreement with the actual measurement results. Furthermore, the junction temperature of each IGBT dies in the module is almost the same.

4 Reliability estimation for automotive application

4.1 Driving pattern and reliability of the IGBT module for automotive

The required reliability level of the IGBT modules for the automotive application is higher than that of the industrial application. For example, the requirement of car lifetime is generally 150,000miles in 15 years [6]. Therefore, it is very important that the reliability estimation based on the driving pattern of traction situation.

Figure 9 shows the example of temperature changes of the IGBT/FWD dies, the pin fin base plate, the cooling liquid, and the ambient based on the driving pattern of traction situation. The ΔT_j is a junction temperature change of IGBT and FWD dies. The ΔT_c is a case temperature change of the cooling pin fin base. The T_w is a cooling liquid temperature. The values of ΔT_j , ΔT_c and T_w depend on the PCU operation condition. The T_a is an ambient temperature and changes by the cycle of the seasonal temperature in a year.

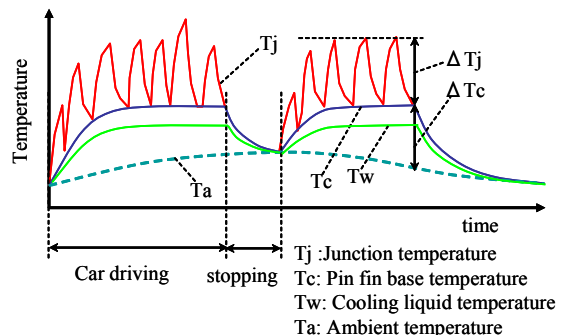


Figure 9: Temperature changes due to driving pattern of traction situation.

From the temperature change of several parts shown in Figure 9, the ΔT_j power cycling test and the ΔT_c power cycling test (Thermal Fatigue life Test) are very important in the IGBT module for the automotive application. In addition, the thermal cycling test without electrical stressing is also important in the IGBT module for the automotive application. The required cycling numbers for thermal cycling test is generally more than 1,000 cycles.

The reliability estimation is carried out by using a temperature profile based on the typical driving pattern [7], [8], and by modeling the temperature cycle in automotive usage [6]. We have studied the simple estimation method of the ΔT_j and the ΔT_c

power cycling lifetime by considering the operation condition of the IGBT module in the PCU system.

4.2 Calculation of the power dissipation loss, ΔT_j and ΔT_c

Firstly, the power dissipation loss of the IGBT module from the device characteristics and the PCU operation conditions is calculated to estimate the reliability and lifetime. Then, ΔT_j and ΔT_c are calculated from the power dissipation loss results and thermal resistance of the IGBT module. The acceleration and braking conditions are applied for the IGBT and FWD parts calculation respectively. The temperature change based on the abnormal operation conditions, such as rotor-locked operation and short-circuit operation are not considered in this estimation.

Table 2 shows the assumed operation conditions of PCU for the power dissipation loss calculation of the newly developed 650V/400A IGBT module.

Table 2: Operating conditions for new developed 650V/400A IGBT module.

Items	Conditions	Unit
Application	3 phase inverter	-
Bus voltage between P/N terminals	300	V
Rated output current (rms value)	100	A
Maximum output current (rms value)	200	
Carrier frequency	10	kHz
Power factor ($\cos \phi$)	+/-0.9	-

4.3 Required ΔT_j and ΔT_c power cycling lifetime

For the estimation about the ΔT_j and the ΔT_c power cycling lifetime, the required numbers of the ΔT_j and the ΔT_c cycles in the car lifetime should be defined. Table 3 shows the required number of cycles about the ΔT_j and the ΔT_c power cycling test, these numbers are assumed in consideration of the car driving operations and car lifetime. The detail of assumption process of these required cycles are shown in Table 4. The power module must have longer life time than these numbers.

Table 3: Required number of cycles about ΔT_j and ΔT_c power cycling test

Driving Operation Cases		Estimated maximum temperature change, ΔT_j and ΔT_c [°C]	Required cycles [cycle] (operation ratio)
1	Cold start in winter	$T_c = -20$ to 80	100 3×10^3 (25%)
2	Cold start in other seasons	$T_c = 20$ to 80	60 9×10^3 (75%)
3	Rated output current operation	$T_j = 80$ to 125	45 2×10^6 (90%)
4	Maximum output current operation	$T_j = 80$ to 150	70 2×10^5 (10%)

Table 4: Assumption process of the required cycles about ΔT_j and ΔT_c power cycling test

<u>Step 1. Car lifetime:</u> 15years 150,000 miles (24.2×10^4 km) ↓
<u>Step 2. Average driving speed:</u> 20km/h ↓
<u>Step 3. Driving operation time per day:</u> 24.2×10^4 km \div 20km/h \div 15years \div 365days $= 2.2$ hour/day ↓
<u>Step 4. Periods of ΔT_j and ΔT_c cycle time :</u> • Period of ΔT_j cycle time : 3 times per 1 minute • Period of ΔT_c cycle time : 1 time per 1 hour ↓
<u>Step 5. Total number of ΔT_j and ΔT_c cycles in car lifetime :</u> • Numbers of ΔT_j cycles: 3 times \times 60minutes \times 2.2hours \times 365days \times 15years $= 2.2 \times 10^6$ cycles • Numbers of ΔT_c cycles: 1 time \times 2.2hours \times 365days \times 15years $= 1.2 \times 10^4$ cycles ↓
<u>Step 6. Operation ratio :</u> • Cold start in winter: 3 months per year (25%) • Cold start in other seasons : 9 months per year (75%) • Rated output current operation : 90% in car lifetime • Maximum output current operation : 10% in car lifetime ↓
<u>Step 7. Calculation results of the required cycles :</u> • The required cycles of each cases are shown in Table 3

Firstly, ΔT_c power cycling lifetime is considered. The biggest change of the ΔT_c is observed in winter, and the lowest ambient temperature in human dwelling area may be -20°C in practice (the case 1 in Table 3). The maximum of the pin fin base temperature T_c is supposed to be 80°C , this value is based on the maximum cooling liquid temperature is $T_w=65^{\circ}\text{C}$ and the temperature difference between T_c and T_w is 15°C . The temperature difference is based on the calculation results of the power dissipation loss and the

thermal resistance $R_{th(c-w)}$ value between the pin fin base and cooling liquid. Therefore, the estimated maximum ΔT_c is 100°C and the required number of cycles is 3×10^3 cycles in the case 1.

In other seasons, the average ambient temperature is assumed to be 20°C . The case 2 in table 3 is in this case. The maximum of the T_c is supposed to be 80°C , too. Therefore, the estimated maximum ΔT_c is 60°C and the required number of cycles is 9×10^3 cycles in the case 2.

The period of the ΔT_c cycle time is assumed 1 hour by considering the time which the vehicle cools fully.

Next, ΔT_j power cycling lifetime is considered. The case 3 and 4 are related with the estimation of the ΔT_j power cycling lifetime. The temperature changes of the IGBT and FWD dies depend on various drive conditions, such as acceleration, braking, flat level road, uphill or downhill roads, traffic jam, suburban or expressway driving, and so on. Therefore, it is difficult to define the temperature change simply at the various driving conditions.

In this paper, the required ΔT_j power cycling lifetime is simply estimated from the rated power and the maximum power of PCU operation conditions. We have assumed that the driving operation conditions are distinguished the two cases. The one is the case 3, which corresponds to the normal driving conditions such as the flat level roads with the rated output power shown in Table 2. And the other is the case 4, which corresponds to the rapid acceleration and the sudden braking driving operations, for example, with the maximum output power shown in Table 2.

The period of the ΔT_j cycle time and the operation ratio of the rated and the maximum power are assumed in consideration of the typical human driving operation pattern. The operation ratio of the rated power and the maximum power is assumed to 90% and 10%. The total required number of ΔT_j power cycle is 2.2×10^6 cycles. Therefore, the required ΔT_j cycle in case 3 is 2.0×10^6 , and in case 4 is 2.0×10^5 .

4.4 Estimation and actual results about reliability for the newly developed IGBT module

For the estimation of the ΔT_j and the ΔT_c power cycling lifetime, the estimated ΔT_j and ΔT_c power cycling lifetime curves are needed. Figure

10 and 11 show the estimated ΔT_j and ΔT_c [6] power cycling lifetime curve of the newly developed IGBT module. The tin(Sn) and antimony(Sb) solder system [6] is applied under the insulated substrate.

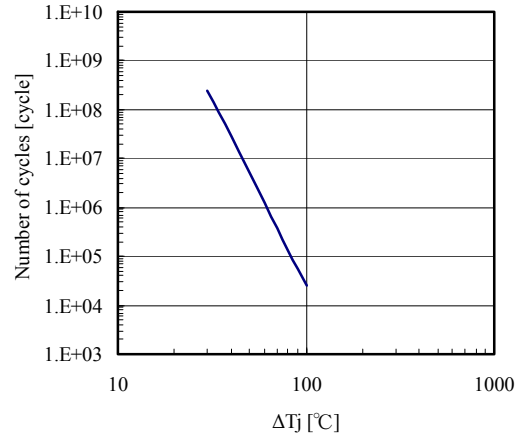


Figure 10: Estimated ΔT_j power cycling lifetime curve

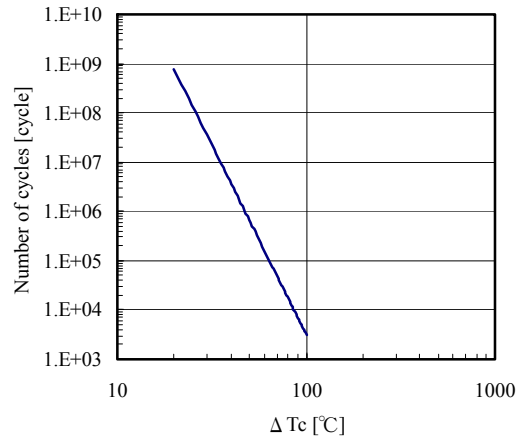


Figure 11: Estimated ΔT_c power cycling lifetime curve [6]

Table 5 shows the estimation results about the ΔT_j and the ΔT_c power cycling lifetime from the ΔT_j and ΔT_c lifetime curves (Figures 10 and 11) for each temperature cycles in Table 3. The numbers of the estimated power cycling lifetime about the ΔT_j and the ΔT_c power cycle test are beyond the required cycles in the each driving operation cases shown in Table 3. Furthermore, the sum of the ratio of a) to b) in the ΔT_j power cycle test and the ΔT_c power cycles test are under 100%. Therefore, the ΔT_j and the ΔT_c power cycling lifetime of the newly developed IGBT module are enough to satisfy the requirement of the automotive application.

Table 5: Estimation results about ΔT_j and ΔT_c power cycling lifetime

Power cycle test and driving conditions		ΔT_j and ΔT_c [°C]	a) Required cycles [cycles] (operation ratio)	b) Estimation result of power cycling lifetime [cycle]	Ratio of a) to b) [%]
ΔT_c power cycle	Winter	100	3×10^3 (25%)	3.7×10^3	81
	Other seasons	60	9×10^3 (75%)	1.1×10^5	8
ΔT_j power cycle	Rated output current operation	45	2×10^6 (90%)	1.1×10^7	18
	Maximum output current operation	70	2×10^5 (10%)	3.8×10^5	53

Figure 12 shows the relative thermal resistance change depend on the number of the temperature cycles for the new developed 650V/400A IGBT module. The tested temperature change condition is 165°C (-40 to 125°C). The relative thermal resistance is not increased to the point of 1,000 cycles. The temperature cycle reliability of the newly developed IGBT module is satisfied for the automotive application.

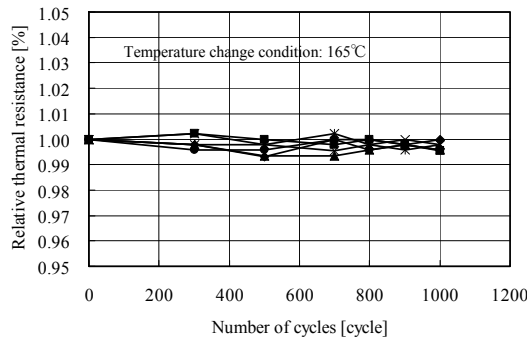


Figure 12: Relative thermal resistance change in temperature cycle test

4.5 Decrease of the crack area in solder layer under the insulated substrate

It is important that the decrease of the crack area in solder layer under the insulated substrate for the purpose of improving the ΔT_c power cycling and temperature cycling lifetime [9]. The SiN insulated substrate is applied for the newly developed 6-pack IGBT modules.

Table 6 shows the typical values of the thermal conductivity and the thermal expansion coefficient of the aluminum oxide and the silicon nitride compared with the copper. The silicon nitride has a higher thermal conductivity than that of the aluminum oxide. Therefore, high

thermal performance in the IGBT module is expected by using the silicon nitride for the insulated substrate.

On the other hand, the thermal expansion coefficient of the silicon nitride is lower than that of the aluminum oxide. Therefore, the difference of the thermal expansion coefficient against the copper fin base is larger, and the crack in the solder layer under the insulated substrate will be occurred easily. We have applied the tin(Sn) and antimony(Sb) solder system to reduce the occurrence of cracks in the solder layer under the insulated substrate [6]. Several kinds of Sn-Sb solders were investigated to optimize the melting temperature and the module reliability.

Table 6: Thermal conductivity and thermal expansion coefficient

Materials	Thermal conductivity [W/mK]	Thermal expansion coefficient [ppm/K]
Aluminum oxide	20	7
Silicon nitride	70	3
Copper	390	16

Figure 13 shows the comparison of the relative crack length under the insulated substrate with various Sn-Sb solders upon the temperature cycle test. The relative crack length is the ratio of the crack length from the corner to the diagonal of the insulated substrate.

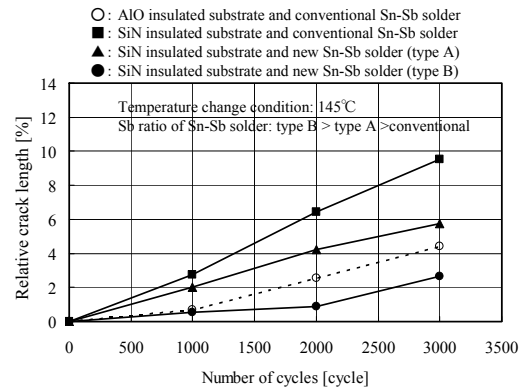


Figure 13: Growth of crack length in the Sn-Sb solder layer under the insulated substrate

Figure 14 shows the typical ultrasonic photo of the test piece after 3,000 temperature cycles. The white areas indicate the crack growth inside the solder layer under the insulated substrate. The temperature change condition is 145°C (-40 to 105°C).

In the case of the SiN insulated substrate, the relative crack length is reduced below that of the conventional AlO insulated substrate by increasing the ratio of the antimony in Sn-Sb solder. The increase of Sn-Sb bonding reduces the crack growth in the solder layer under the insulated substrate. We have optimized the amount of antimony in Sn-Sb solder in consideration of the melting temperature of the Sn-Sb solder. We have achieved the reliability of the newly developed IGBT modules by the optimized Sn-Sb solder for the automotive application.

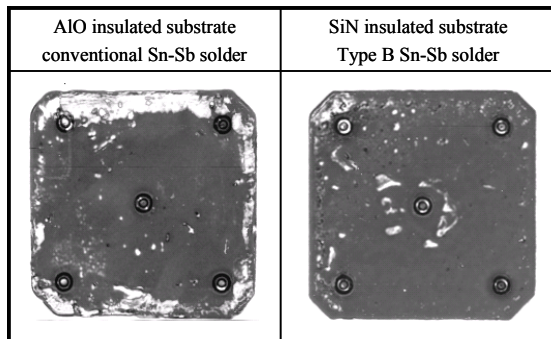


Figure 14: Ultrasonic photos of the Sn-Sb solder layers after 3,000 temperature cycles

5 Conclusion

In this paper, the newly developed 6-pack direct liquid cooling IGBT module for the automotive application is described. The direct liquid cooling fin and the cooling liquid jacket structure have been optimized to achieve high thermal conductivity.

The several Sn-Sb solder materials under the insulated substrate have been investigated with temperature cycling test and the amount of antimony(Sb) has been optimized to reduce crack growth in the solder layer under the insulated substrate.

From the estimation of the ΔT_j and the ΔT_c power cycling lifetime and several reliability test results, the reliability of the newly developed IGBT modules with the optimized Sn-Sb solder has been achieved the requirement for the automotive application.

In conclusion, the newly developed direct liquid cooling IGBT module and the optimized cooling liquid jacket can reduce the size of PCU in HEV/EV system against the conventional fin less base type 6-pack IGBT modules.

4 References

- [1] F. Nagaune et al., Small Size and High Thermal Conductivity IGBT Module for Automotive Applications, ISBN 978-3-8007-3344-6, Proceedings PCIM Europe 2011 conference (2011), 785-790
- [2] H.Nakano et al., 600V trench-gate IGBT with Micro-P structure, ISBN 978-1-4244-3524-1, Proceedings of the 21th International Symposium on Power Semiconductor Devices and ICs (2009), 132-135.
- [3] K.Sasaki et al., Small Size, Low Thermal Resistance and High Reliability Packaging Technologies of IGBT Module for Wind Power Applications, ISBN 978-3-8007-3229-6, Proceedings PCIM Europe 2010 conference (2010), 267-272.
- [4] Dr. Dusan Graovac et al., Power Semiconductor Solutions for Electric Vehicles, Proceedings of the 25th World Battery, Hybrid and Fuel Cell Electric Vehicle Symposium & Exhibition, (EVS-25 Shenzhen, China, Nov. 5-9, 2010).
- [5] T.Kurosu et al., Packaging Technologies of Direct-Cooled Power Module, ISBN 978-1-4244-5395-5, Proceedings of the 2010 International Power Electronics Conference (2010), 2115-2119
- [6] A. Nishiura et al., Improved life of IGBT module suitable for electric propulsion system, Proceedings EVS24 International Battery, Hybrid and Fuel Cell Electric Vehicle Symposium, (EVS-24 Stavanger, Norway, May 13-16, 2009)
- [7] A. Christmann et al., Reliability of Power Modules in Hybrid Vehicles, ISBN 978-3-8007-3158-9, Proceedings PCIM Europe 2009 conference (2009), 359-366.
- [8] A. Christmann et al., Facing high thermal loads on Power Modules in Hybrid Electrical Vehicles, ISBN 978-3-8007-3229-6, Proceedings PCIM Europe 2010 conference (2010), 432-438.
- [9] A. Morozumi, et al., "Reliability of power cycling for IGBT power semiconductor modules", IEEE TRANSACTIONS ON INDUS-TRY APPLICATIONS. Vol.39,

Authors



Fumio Nagaune received the M.E. degrees in electric engineering and the D.E. degrees in Material engineering from Shinsyu University, Nagano, Japan., in 1987 and 2002, respectively. In 1987, he joined Fuji Electric Co., Ltd. He is currently developing a IGBT modules for EV/HEV applications.



Shinichiro Adachi received the M.E. degrees in semiconductor engineering, from Kyushu University, Fukuoka, Japan, in 2010. In 2010, he joined Fuji Electric Co., Ltd. He is currently developing a IGBT modules for EV/HEV applications.



Takahisa Hitachi received the B.E. degrees in electric and electronics system engineering, from Yamanashi University, Yamanashi, Japan, in 2006. In 2006, he joined Fuji Electric Co., Ltd. He is currently developing a IGBT modules for EV/HEV applications.



Hiromichi Gohara received the M.S. degree in Intelligence mechanical engineering speciality from Tokyo Denki University, Saitama, Japan, in 2004. In 2004, he joined Fuji Electric Co., Ltd. He is currently developing a high heat dissipation and a high-reliability module structure for EV/HEV applications.



Akira Morozumi received the B.S. degree in metallurgical engineering from Chiba Institute of Technology, Chiba, Japan, in 1988. In 1991, he joined Fuji Electric Co., Ltd. He is currently developing a high reliability module structure for EV/HEV applications.



Akira Nishiura received the M.E. degree in Physical engineering from Tsukuba University, Ibaraki, Japan, in 1983. In 1983, he joined Fuji Electric Co., Ltd. Since 2002, he is the head of development section of IGBT Module for EV/HEV applications.